Development and Implementation of an Autonomous Solar-Powered Drone for Disaster Relief

[1] Vu Ngoc Kien, [2] Trương Minh Bao Anh
[1] *Vietnam Academy of Military Science and Technology*
[2] *HUS High School for Gifted Students, University of Science, Vietnam*
Corresponding author: Vu Ngoc Kien
Email: kvu3009@gmail.com

Abstract

Introduction: Disaster relief operations face significant challenges in assessing and responding to emergencies in hazardous environments. Traditional methods often struggle due to limited access, power constraints, and operational risks. Autonomous drones offer a promising solution, but their reliance on battery power limits their operational duration.

Objectives: This study focuses on developing a novel Solar Sentinel-Disaster Drone X (SS-DDX) equipped with a solar power system and an intelligent deep learning model for efficient human detection in disaster areas.

Methods: The SS-DDX utilizes an ArduPilot Mega flight controller for autonomous navigation, a 3500mAh Lithium-Ion battery for power, and a 50W flexible solar panel for extended flight endurance. The drone employs a GoPro Hero 10 camera to capture high-resolution images of disaster zones. A Relief Vision Deep Convolutional Neural Network (RVDCNN) model integrated with the Intelligent Zebra Optimization (IZO) algorithm (IZ-RVDCNN) is developed to detect humans in the captured images. Data preprocessing techniques, including Min-Max normalization and Histogram of Oriented Gradients (HOG) feature extraction, enhance model performance.

Results: The IZ-RVDCNN model demonstrates high accuracy (91%), precision (91.70%), and recall (98%) in human detection, significantly outperforming existing methods.

Conclusions: The SS-DDX represents a significant advancement in disaster relief operations, offering increased autonomy, extended flight duration, and enhanced human detection capabilities. The study highlights the potential of solar-powered drones and intelligent deep learning algorithms in improving response efficiency and saving lives in disaster situations.

Keywords: Disaster Relief Operations, Relief Vision- Deep Convolutional Neural Net (RV-DCNN), Solar Sentinel-Disaster Drone X (SS-DDX), Solar-Powered Drone, Camera Data.

1. Introduction

It is very important to respond appropriately and quickly following natural disasters to minimize loss of life and damage. This is just but the area of operation of the disaster which weather, a wider area, or restricted access to the affected region is among the many challenges that are usually faced by the traditional modes of disaster aid (ElSayed et al., 2023). So, institutional-owned autonomous drones have emerged as a plausible solution that can offer the capability to quickly and efficiently assess disaster areas deliver required goods and services, are capable of helping with the search and rescue missions (Chu et al., 2021). Some of the weaknesses include the fact that conventional drones can only work for some time in large or isolated disaster areas due to the reliance on restricted energy sources.

The development of an independent flying machine charged with the solar system is suggested to be a significant contribution to the organization of disaster relief to solve this issue. These drones may provide coverage of disaster areas for more extended periods using solar power to enhance the operational autonomy and flight endurance of drones (Saravanan et al.,2024). This innovation removes the necessity of battery replacement or recharging which is mostly unamenable during an emergency, in circumstances where there are power blackouts or breakdown of

physical transportation infrastructure Lin et al., (2024). Solar-powered drones with self-guidance capability allow for constant surveillance missions in real-time without having to be physically operated by man.Dispatch of vital data on vital statistics to emergency response units, large area aerial surveys, transportation and delivery of food, water, and medical supplies to the storm-ravaged or difficult terrains, and other such operations are accomplished using these drones (Hima and Thampatty, 2023). They can also accommodate complex sensors and imaging apparatus that facilitate the dispensation of aid by helping to map out the area, assess the extent of the disaster as well as identify people who might have been alive throughout the disaster (Alawad et al.,2023).

The aspects, operating energy, and construction of the self-governing solar-powered drone for disaster relief are deliberated. It highlights how the endurance of the drones and their ability to navigate and carry loads can be enhanced through the integration of solar energy systems with self-regulating algorithms Cai and Liang, (2023). There is great potential in the use of this technology because while minimizing the environmental impact of disasters, it also enhances the efficacy of relief operations. Solar-powered drones remain the most sustainable solution, and in many cases, they address some of the most significant issues in disaster management through the use of autonomous systems and renewable energy (Kamal et al., 2023).

In this work, we design a new concept SS-DDX with an integrated ArduPilot Mega flight controller. Specifically, this controller relies on the mission planner 2 configuration. 1. 101 to effectively organize flight courses as well as utilize is known as IZ-RVDCNN for identifying human presence in the disaster area.

In Section 2, a list of literature reviews is provided. In Section 3, the approach is explained. The Findings include a mention of Section 4. In Section 5, the conclusion is provided.

2. Related works

A hexcopter for surveillance and monitoring purposes has been built and presented by (Hassan et al., 2021). A highly versatile and adaptable platform was offered by the technology for uses such as aerial imagery and surveillance. Governmental organizations, military uses, disaster relief efforts, and other purposes were all eligible for utilizing equipment.

As an efficient remedy for communication loss after a natural disaster, Padilla et al.,(2020) created an aerial communication relay platform. Signal quality improved as compared to the non-optimized situation, according to the results of the optimal flight path simulation.

A solar-powered unmanned aerial vehicle (UAV) exploring several safety and recovery locations in a mountainous area faced a path planning difficulty that was investigated by (Huang and Savkin, 2021). The procedure was meant for a single UAV. Another area of research was creating techniques for many UAVs to further enhance the time it takes to locate a target.

(Chaudhary et al., 2021) investigated the possible application of drones in natural disaster situations such as floods, cyclones, earthquakes, and volcanic eruptions, not just for searching victims, animals, and significant items. They attempted to decrease the number of obstacles that prevent UAVs from being deployed effectively and to extend the flying time for the rescue mission.

A model for organizing an inspection trip was proposed by (Huang and Savkin, 2021) solar-powered UAV takes off from its base, travels to a predefined route, and then returns to the storage while preserving its remaining energy and avoiding collisions with mountains. The proposed route planning technique first identified a suitable inspection path based on quickly exploring random trees (RRT) that enabled the UAV to complete its task.

The design and development of an autonomous drone system was the main purpose of the investigation by (Kalta et al., 2024) which showed how it has the potential to transform several industries and enhance sustainability, efficiency, and safety when applied morally and responsibly. Successful autonomous flying demonstrations that highlight the drone's capability to finish challenging missions would be among the outcomes.

Bibliometric evaluation of post-disaster building damage evaluation and inspection methods was conducted by (Al Shafian and Hu, 2024) on the key advances and problems in the critical issue. The outcomes showed notable improvements in data gathering and processing techniques, highlighting the value of machine learning and remote sensing in augmenting assessments of disaster damage.

3. Methods

The images gathered in disaster regions and to improve data quality, images were normalized using Min-Max normalization. The HOG approach, which prioritized edges and gradients for efficient human identification, was used to extract features. During search and rescue operations, this procedure enhanced the IZ-RVDCNN performance.

3.1. Data collection

To achieve optimal performance in disaster relief missions, components had to be chosen and integrated throughout the hardware design process for the SS-DDX. First, the ArduPilot Mega flight controller was integrated. It was set up to use Mission Planner 2.1.101 to operate the drone's autonomous navigation. The drone was able to fly over disaster zones precisely due to this configuration.Brushless DC motors were linked to 30-amp electronic speed controllers (ESCs) for reliable flight and propulsion. These motors were picked because they were effective and were put through testing to make sure could generate the thrust required to maneuver across difficult terrain. An integrated 3500mAh Lithium-Ion battery functioned as the drone's main power source. A 50W flexible solar panel was added to this to enable in-flight recharging and increase operating duration. The efficacy of the solar panel in maintaining the drone's electricity throughout prolonged missions was verified by testing in a range of sunshine situations.The GoPro Hero 10 camera was set up to collect data by taking high-definition images and videos of the disaster region. The camera was put to the test to see how well it captured images in various lighting and debris-filled environments. The SS-DDX was particularly successful for search and save operations in disaster-affected situations because of its hardware configuration, which guaranteed its ability to operate for extended periods and capture images efficiently.

3.2. Data pre-processing using min-max normalization

By removing scale biases during processing, Min-Max normalization modifies input variables to improve model performance and provide consistency across features for identifying persons in disaster zones.

This is the most straightforward normalization method that not only gets the scores into the standard numerical range of [0, 1] but also keeps the original distribution shapes aside from a scaling factor. For each matcher, let W represent the set of raw matching scores. Afterwards, w'represents the normalized score for w. The maximum and minimum values of the raw matching scores are represented by max (W) and min(W), respectively. Following that, the normalized score is determined as equation 1.

$$w' = (w - \min(W)/\max(W) - \min(W)) \quad (1)$$

This approach is not robust since it is extremely susceptible to outliers in the estimation data. The majority of the data only concentrates on a smaller range due to the existence of outliers.

3.3. Feature extraction using HOG

Focusing on human-specific characteristics in the chaotic environment, these extracted features aid algorithms in differentiating persons from other objects or particles, increasing search and saving mission effectiveness.

The field of computer vision has effectively employed the HOG descriptor. It has mostly been applied to the identification of objects, people, and pedestrians. Magnitude and orientation are used to calculate HOG. The input image's horizontal and vertical gradients are calculated using the following equations, 2 and 3.

$$H_w = J_e * [-1, 0, 1] \quad (2)$$

$$H_z = J_e * [-1, 0, 1]^S \quad (3)$$

Using equations 4 and 5, gradients thus generated are then used to determine gradient magnitude and angular orientations.

$$n(w,z) = \sqrt{h_u^2(w,z) + h_g^2(w,z)} \quad (4)$$

$$\theta(w,z) = tan^{-1}\left(\frac{h_u(w,z)}{h_g(w,z)}\right) \quad (5)$$

The image is divided into cells by it. A block made up of different cells is generated, and the blocks are convolved to create features.

There is an overlap between these blocks. Quantized orientations about the same cell are combined into the final histogram bins. After sorting, these histogram bins are combined to create the final histogram. The

total amount of features computed using the HOG descriptor is represented byS_{hog_fs}. Block size is expressed by A_t, while the number of bins used is indicated by M_a. A_{img}stands for blocks per image. The total amount of features can then be calculated using the formula found in Equation 6.

$$S_{hog\_fs} = A_{img} * A_t * M_a \quad (6)$$

Recognizing the humans in the disaster area

This model improves detection performance and efficiency by fusing a Deep Convolutional Neural Network (RVDCNN) depending on Relief Vision with the Intelligent Zebra Optimization (IZO) algorithm. This is especially important in disaster situations because survivors must be found quickly and adaptably amid the chaos and wreckage. To achieve fast convergence towards the best solution, the IZO algorithm simulates zebra herd intelligence and improves the learning process. Meanwhile, the algorithm makes sure that only the most pertinent features are chosen, eliminating noise and unnecessary data in the process.The RVDCNN architecture is particularly effective at extracting meaningful patterns and identifying human forms amidst chaos or rubble in catastrophe settings when complex visual cues and barriers can make detection more difficult.This model improves accuracy and efficiency in human detection amidst disaster-related complications by combining the IZO method with a fine-tuned RVDCNN. This allows the model to make use of the resilience of zebra-inspired optimization and the power of deep learning. The hybrid model, IZ-RVDCNN, performs particularly well in real-time human recognition during disaster relief efforts. It offers improved detection accuracy, shorter reaction times, and reliable performance in difficult environments where standard models struggle.

RVDCNN

RVDCNN architecture improves the accuracy of detecting survivors by effectively capturing features from a variety of environmental circumstances. Identify humansin disaster region more quickly and effectively with the help of this creative strategy, which ultimately saves lives.

The input image size is set to 224 × 224 × 3 based on the experience and computational power of the machine. It is composed of many depth-directed slices. Numerous neurons are represented by a single slice, and the convolution kernel (CK) a square filter can be compared to the number of neurons, such as 16 x 16, 9 × 9, or 5 × 5. The purpose of these neurons is to extract the feature of the immediate area in the image that they each belong to. Assuming that the input image size is X, the CK size is E, and the mobile stride of the CK is T (usually T = 2), we can calculate the dimension of the image after convolution as $(X - E + 2O)/T + 1$. Padding O is used to complete the boundary of the supplied imageoften O = 0. The output tensor is then obtained.

- **DCNN**

Three convolutional layers make up the hierarchical architecture of DCNNs. Different low-level characteristics, such as edges, lines, and corners, are extracted from the input image using the first convolutional layer. High-tier features are available to the other two figure 1 shows the architecture of DCNN.

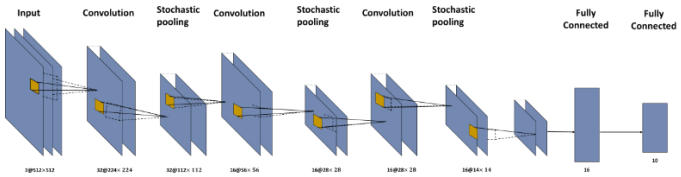

Figure 1: Architecture of DCNN

Every output map features convolutional mixes of many input maps. In general, the output can be represented by the formula that follows in equation 7.

$$w_i^k = e\left(\sum_{j \in N_i} w_i^k * l_{ji}^k + a_i^k\right) \quad (7)$$

Herea_i stands for bias, $l_{ji}$for CK for the lth layer, and N_i for a collection of input maps. In the technical implementation of DCNNs, an additive bias can be introduced in addition to sigmoid or $tanh$ functions. The amount of the unit at the place, for instance, (w, z)in the jthlayer, and the feature map, designated asu_{ji}^{wz}, is provided by equation 8.

$$u_{ji}^{wz} = signmoid\left(a_{ji} + \sum_{o=0}^{O_j-1} \sum_{r=0}^{R_i-1} x_{ji}^{or} u_{(j-1)}^{(w+o)(z+r)}\right) \quad (8)$$

Where $O_j$and $R_i$are the kernel's height and width, sigmoid $(\cdot)$ is the sigmoid function, $a_{ji}$is the feature map's bias, and x_{ji}^{wz} is the kernel weight (KW) number at the point (o, r)associated with the layer. DCNN variables, such as bias$a_{ji}$and KW x_{ji}^{or}, are often learned by unsupervised methods.

- **Stochastic pooling layer (SPL)**

In DCNNs, replace the sub-sampling layer with an SPL. The SPL, which may calculate a feature's maximum value across an area of the image, is used to lower variation. Even if there are slight differences in the image features, the outcome will remain the same. Stochastic pooling avoids over-fitting in addition to combining the benefits of max-pooling and meaning-pooling. It is crucial for the disaster relief operations.

To begin with, it must use Equation (9) to calculate the probability o for every region i in stochastic pooling.

$$o_j = \frac{\alpha_j}{\sum_{l \in Q_i} \alpha_l} \quad (9)$$

Here i is the index of every component within it and Q_i is the pooling region j in feature map$d$,to choose a location k inside the region, then sample from the multinomial distribution depending on $o$stochastic (s) which stands for the stochastic pooling operation, defined as follows for each feature map d.

$$\alpha_{o,r}^{k,l} = Stochastic_{(n,m,j,i) \in o}\left(\alpha_{n,m}^{k-1,l} v(j,i)\right) \quad (10)$$

Here $v(j,i)$ is the weighting frame variable, and $\alpha_{o,r}^{k,l}$ is the neural activation at the location (o,r)in feature map L in the k_{th} layer.

The solution offers the benefit of an SPL, which accelerates DCNN convergence and enhances their capacity for generalization when handling superior invariant information.

- **Softmax regression**

When solving multi-class classification problems, softmax regression is used. The form that the hypothesis functions takes equation 11.

$$g_\theta(w) = \frac{1}{1+\exp\left(-\theta^S w\right)} \quad (11)$$

To minimize the cost function $I(\theta)$by training θ

$$I(\theta) = -\frac{1}{n}\left[\sum_{j=1}^{n}\sum_{i=0}^{k} k\{z^{(j)} = i\} log o(z^{(j)} = i|w^{(j)};\theta)\right] \quad (12)$$

$z^j \in \{1,2,\ldots.,l\}$ for the training dataset$\{w^{(1)}, z^{(1)}, \ldots\ldots, (w^{(n)}, z^{(n)})\}$. The possibility that w will be classified as a category i in Softmax regression is equation 13.

$$o\left(z^{(j)} = i|w^{(j);\theta}\right) = \frac{e^{\theta_l^S w^{(j)}}}{\sum_{k=1}^{l} e^{\theta_k^S w^{(j)}}} \quad (13)$$

A technique for supervised learning is used for developing the connection. The similarity between training samples is reflected in the internal representation. To identify a person's maximal activation neurons reflect the known human, and this knowledge is necessary to understand the feature representation acquired by the DCNN. Finally, by averaging image patches connected to the neurons in a higher layer with stochastic responses, we visualize the image features.

- **Training algorithm**

Furthermore, train DCNNs with the back gradient-descent method. There are two feedforward pass (FFP) stages and one back propagation pass(BPP) stage in it. We discuss an FFP stage multiclass issue with d categories and M training instances. Equation 14 can be used to find the squared error value.

$$F^M = \frac{1}{2}\sum_{m=1}^{M}\sum_{l=1}^{d}(s_l^m - z_l^m)^2 \quad (14)$$

The lthcomponent of the corresponding label for themthsequence is denoted by s_l^m and the quantity of the lthoutput layer unit in reaction to the mthinput sequence is represented byz_l^m.

Let k stand for the current layer(CL), K for the output layer(OL), and l for the input layer(IL). The CLs output is specified as equation 15.

$$w^k = sigmoid(X^k w^{k-1} + a^k) \quad (15)$$

Here a stands for bias and X for the weight value matrix.

When moving from the upper to the lowest layers in equation 16, the back-propagated mistakes can use a subsequent recurrence function around the BPP stage.

$$\delta^k = (X^{k+1})^S \delta^{k+1} \odot e'(X^k w^{k-1} + a^k) \quad (16)$$

Where$\odot$ stands for the multiplication of elements, it will update the weight using the equations 17and 18below.

$$\frac{\partial F}{\partial X^k} = w^{k-1}(\delta^k)^S$$

(17)

$$\Delta X^k = -\eta \frac{\partial F}{\partial X^k}$$

(18)

IZO

IZO enhances situational awareness and expedites rescue operations by optimizing parameters for algorithms that evaluate visual data and quickly identify people in difficult-to-reach environments.

Beginning individuals of tent chaotic mapping

The Zebra Optimization Algorithm (ZOA) generates entirely random individuals of zebras when the individuals are initially established. During the subsequent resolution analyze, the ZOA is expected to decrease into a local optimal resolution because the majority of the initial zebra locations are probably going to be far from the ideal outcome. The initial group of zebras may be distributed unevenly as an effect of this conventional initiation technique. Therefore, to determine the zebra individuals and create more uniformly distributed individuals in the search space, tent chaotic map is employed. The modified initialization equation is as follows in equations 19 and 20.

$$w_j = q_j.(v_a - k_a) + k_a$$

(19)

$$q_j = \begin{cases} \frac{q_{j-1}}{\beta} q_{j-1} \in [0, \beta] \\ \frac{1-q_{j-1}}{1-\beta} q_{j-1} \in [\beta, 1] \end{cases}$$

(20)

Where $q_j$represents the generated chaotic sequence, $w_j$represents the individual zebra following tent chaos startup, v_a, and $k_a$indicate the generable zebra places' top and bottom boundaries, and β is a chaotic parameter that can be changed.

- **Sine cosine approach (SCA)**

To improve the ZOA's ability to explore globally, the SCA was used during the hunting stage to modify the location modify equation 21 of zebra individuals in compliance with the SCA. Following the development of the sine cosine strategy, the following is the revised formula for foraging behavior.

$$w_{j,i}^{m1} = \begin{matrix} w_{j,i} + a_1.\sin a_2.|a_3.Y_i^o - b_2.w_{j,i}|) \; rand < 0.5 \\ w_{j,i} + a_1.\sin a_2.|a_3.Y_i^o - b_2.w_{j,i}|) \; rand \geq 0.5 \end{matrix}$$

(21)

$$a_1 = \left[1 - \left(\frac{s}{S_{max}}\right)^l\right]^{1/l}$$

(22)

Where a_2 and $a_3$are random values generated between$[0,2\pi]$, l is the modification coefficient, and$l \geq 1$.

- **Innovative customizable weight component**

The inclusion of a weight component enhances ZOA's defensive approach by supporting the algorithm's ability to automatically balance its local exploring and global searching abilities. The weight component decreases quickly in the early iterations, aiding in the improvement of each zebra's ability to search globally, while in the intermediate and late iterations, it decreases gradually and softly to reflect the zebras' local exploring in the search space. Below is the dynamic adaptive weight factor (x, y) and updated position update formula for the zebra imperial approach in equations 23 and 24.

$$W_{j,i}^{m2} = \begin{cases} N_1 : x_2.w_{j,i} + 0.01.(2.rand - 1).\left(1 - \frac{s}{S_{max}}\right).w_{j,i}(b_3 \leq 0.5) \\ N_2 : x_2.w_{j,i} + rand.\left(Y_i^B - b_2.w_{j,i}\right)(b_3 > 0.5) \end{cases}$$

(23)

$$x_2 = -\left[1 + \cos\left(\frac{3}{2}\pi + \frac{1}{2}\pi.\frac{s}{S_{max}}\right)\right]$$

(24)

The unique optimization procedure of the IZOA, tent chaos mapping is used to initialize IZOA, and iterative optimization is achieved by combining the defensive formula with a dynamic weighting factor and the foraging equation with a SCA.

- Establish the IZOA population variables, such as the maximum amount of iterations, dimensionality, and zebra count.
- Use tent mapping to start the zebra population.
- Determine each zebra's fitness value individually and note the ideal zebra locations.

- Update each zebra's position by applying the SCA foraging equation
- Create the random numberb_3, and then choose the defensive strategy based on b_3. If$b_3 \leq 0.5$, the zebra updates its location using approachN_1in the modified equation (32) and adds weightscomponents if$b_3 > 0.5$, the zebra updates its location using approachN_2.
- Determine each zebra's fitness value, to update its position, and record the globally optimal solution.
- Ascertain if the criterion for the iteration's termination has been met. If the requirements are satisfied, the global maximum strategy is generated and the IZOA is completed. The loop iterates if the termination condition is not met.

4. Results

The experimental environment and setup, as well as the effectiveness of the suggested approach displayed in Table 1, are covered in this section. Compared with the existing approaches which areYou Only Look Once (YOLO) (Sarosa et al., 2021), Table 2 shows the overall performances.

Table 1: Experimental setup

Experimental Setup	Details
Model	IZ-RVDCNN
Task	Autonomous Solar-Powered Drone for Disaster Relief Operations
Hardware	Laptop running Windows 11
Processor	Intel i7 12th Gen
RAM	16 GB
Software Environment	Python 3.10.1
Evaluation Metrics	Accuracy, precision, recall

Table 2: Overall result comparison

Methods	Accuracy %	Precision %	Recall %
YOLO(Sarosa et al., 2021)	89%	90.82%	97.8 %
IZ-RVDCNN[Proposed]	91%	91.70%	98%

4.1 Overall processing time

Subsequently categorize and identify people to guarantee prompt and precise detection. For prompt response and successful search, these processes must be optimized.Figure 2 shows the output of overall processing time.

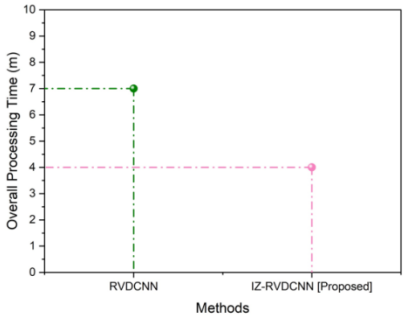

Figure 2: Output of overall processing time

While the RVDCNN achieved 7minutes (m) respectively, our proposed IZ-RVDCNN methodology achieved (4m). The outcome indicates that our suggested approach outperforms.

4.2 Accuracy

It assesses how well detection systems work, which is important for rescue operations since it guarantees accurate identification and reduces false negatives.Figure 3 shows the result of accuracy.

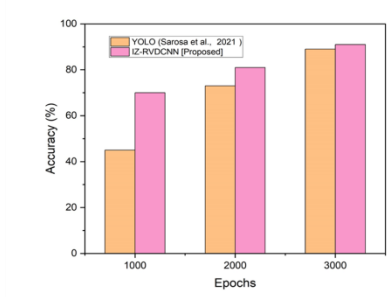

Figure 3: Result of accuracy

While the existing methods YOLO achieved 89% respectively, our proposed IZ-RVDCNN methodology achieved (91%). The findings demonstrate that our suggested approach outperforms existing methods substantially.

4.3 Precision

To ensure that true positives are increased and false positives are minimized for efficient rescue operations, it assesses the recognition system's performance. Figure 4 shows the result of precision.

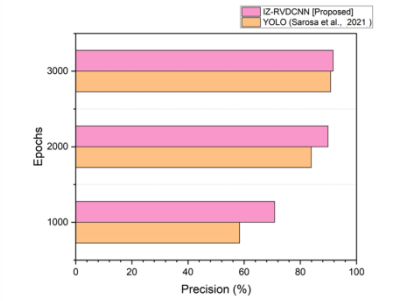

Figure 4: Result of precision

The IZ-RVDCNN technique accomplished a precision of (91.70%), which is admirable to the memory of the traditional methods YOLO (90.82%). The findings indicate that our suggested method outperforms the current techniques by a significant margin in terms of precision.

4.4 Recall

To minimize missed individuals and ensure successful rescue attempts, it computes the ratio of true positive detections to the total number of actual positives.Figure 5 shows the result of the recall.

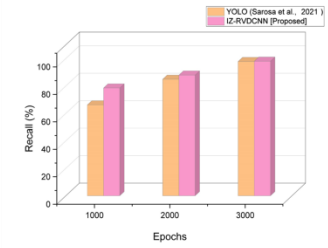

Figure 5: Result of recall

The IZ-RVDCNN technique accomplished a recall of (98%), while traditional methods YOLO achieved (97.8%). The findings indicate that our suggested method outperforms the current techniques by a significant margin in terms of recall.

5. Conclusion

The paper effectively illustrates how the SS-DDX was developed and put into use as a cutting-edge way to improve disaster relief operations. Through the integration of cutting-edge technology, including the IZ-RVDCNN and the ArduPilot Mega flight controller, the SS-DDX demonstrates its potential for efficiently evaluating and handling situations in dangerous environments. The GoPro Hero 10 records and produces high-quality images and videos from disaster zones. This visual information is essential for identifying people and evaluating situations. The data processing methods used,Min-Max normalizationand HOG for feature extraction, have helped the RV-DCNN model achieve remarkable performance metrics, including 91% accuracy, 91.70% precision, and 98% recall. Its drawbacks include the possibility of overfitting because of its intricate design, the need for high-quality training data, sensitivity to changes in the environment, high processing costs, and difficulties with real-time processing, all of which could impair performance during crucial disaster relief operations.Future plans call for improving the effectiveness of the model, integrating it with edge computing for real-time analysis, expanding into other disaster scenarios, incorporating multi-sensor data fusion, and enhancing autonomous navigation to maximize to identification of humans in disaster.

Refrences

[1] ElSayed, M., Foda, A. and Mohamed, M., 2022. Autonomous drone charging station planning through solar energy harnessing for zero-emission operations. Sustainable Cities and Society, 86, p.104122.

[2] Chu, Y., Ho, C., Lee, Y. and Li, B., 2021. Development of a solar-powered unmanned aerial vehicle for extended flight endurance. Drones, 5(2), p.44.

[3] Saravanan, P., Ashwin, G., Arvinth, V.S. and Prasanna, V., 2024, April. Solar Powered Quadcopter Drone. In 2024 10th International Conference on Communication and Signal Processing (ICCSP) (pp. 898-901). IEEE.

[4] Lin, X.H., Bi, S., Su, G. and Zhang, Y.J.A., 2024. A Lyapunov-Based Approach to Joint Optimization of Resource Allocation and 3D Trajectory for Solar-Powered UAV MEC Systems. IEEE Internet of Things Journal.

[5] Hima, M. and Thampatty, K.S., 2023, October. Solar Powered Unmanned Aerial Vehicle. In 2023 7th International Conference on Computer Applications in Electrical Engineering-Recent Advances (CERA) (pp. 1-6). IEEE.

[6] Alawad, W., Halima, N.B. and Aziz, L., 2023. An unmanned aerial vehicle (UAV) system for disaster

and crisis management in smart cities. Electronics, 12(4), p.1051.

[7] Cai, S. and Liang, J., 2023. Joint Optimization of Service Fairness and Energy Consumption for 3D Trajectory Planning in Multiple Solar-Powered UAV Systems. Applied Sciences, 13(8), p.5136.

[8]Kamal, M.V., Dileep, P., Sharada, G., Suneetha, V. and Gayatri, M., 2023. Drone/UAV Design Development is Important in a Wide Range of Applications: A Critical Review. Drone Technology: Future Trends and Practical Applications, pp.53-67.

[9] Hassan, F., Usman, M.R., Hamid, S., Usman, M.A., Politis, C. and Satrya, G.B., 2021, April. Solar powered autonomous hex-copter for surveillance, security and monitoring. In 2021 IEEE Asia Pacific Conference on Wireless and Mobile (APWiMob) (pp. 188-194). IEEE.

[10] Padilla, G.E.G., Kim, K.J., Park, S.H. and Yu, K.H., 2020. Flight path planning of solar-powered UAV for sustainable communication relay. IEEE Robotics and Automation Letters, 5(4), pp.6772-6779.

[11] Huang, H. and Savkin, A.V., 2021. Path planning for a solar-powered UAV inspecting mountain sites for safety and rescue. Energies, 14(7), p.1968.

[12] Chaudhary, S.K., Yadav, A., Sharma, B., Rouf, M. and Gupta, V., 2021, March. RF Controlled Solar Based Robotic Drone. In 2021 International Conference on Advance Computing and Innovative Technologies in Engineering (ICACITE) (pp. 427-431). IEEE.

[13] Huang, H. and Savkin, A.V., 2021. Path planning for a solar-powered UAV inspecting mountain sites for safety and rescue. Energies, 14(7), p.1968.

[14] Kalta, S., Bawa, G., Singh, G., Chauhan, H. and Bag, A., 2024, March. Developing a Prototype for Autonomous Drones. In 2024 3rd International Conference on Sentiment Analysis and Deep Learning (ICSADL) (pp. 702-708). IEEE.

[15] Al Shafian, S. and Hu, D., 2024. Integrating Machine Learning and Remote Sensing in Disaster Management: A Decadal Review of Post-Disaster Building Damage Assessment. Buildings, 14(8), p.2344.

[16] Sarosa, M., Muna, N. and Rohadi, E., 2021, March. Detection of natural disaster victims using You Only Look Once (YOLO). In IOP Conference Series: Materials Science and Engineering (Vol. 1098, No. 3, p. 032076). IOP Publishing.